Predict Locational Marginal Greenhouse Gas Emission Factors of Electricity with Spatial-Temporal Graph Convolutional Networks

Wenyu Wang, Yinglun Li, Nanpeng Yu
Department of Electrical and Computer Engineering
University of California, Riverside
Riverside, CA 92521
wwang032@ucr.edu, yli377@ucr.edu, nyu@ece.ucr.edu

2023 IEEE PES Innovative Smart Grid Technologies Europe (ISGT EUROPE) | 979-8-3503-9678-2/23/$31.00 ©2023 IEEE | DOI: 10.1109/ISGTEUROPE56780.2023.10407422

***Abstract*—The electric power system is a major contributor to greenhouse gas (GHG) emissions. To reduce GHG emissions, accurate emission predictions are essential. The marginal emission factor (MEF) is a useful signal for distributed energy resource aggregators and end-use customers to mitigate GHG emissions by scheduling the flexible loads accordingly. The existing methods of locational MEF prediction often suffer from high computational burden, low prediction accuracy, and low time granularity. In this paper, we propose a hybrid machine learning framework to predict GHG emissions and locational MEF, which integrates feed-forward neural networks with spatio-temporal graph convolutional networks (STGCNs). With the power of STGCN, the proposed framework can capture the spatio-temporal pattern in power grid data. A comprehensive case study in California shows that the proposed approach outperforms the existing techniques in prediction accuracy. The proposed model provides short-term locational MEF predictions with high time granularity using only publicly available dataset.**

***Index Terms*—Greenhouse gas emission, spatio-temporal graph convolutional network, graph neural network, deep learning.**

I. Introduction

Excessive emission of greenhouse gas (GHG) can cause global climate change and notable environment impact, such as global warming and rising sea-levels. Reducing GHG emission is the key to slowing such detrimental processes. The U.S. government has announced a target of 50-52% GHG emission reduction below 2005 levels by 2030 [1]. The electric power system is one of the main contributors of GHG emissions, producing about 25% of the total GHG emissions [2]. In power system operations, a mixture of generation resources are coordinated not only to meet the varying electricity demand with least cost while satisfying a number of operational constraints. Different generation resources have different levels of GHG emissions. Fossil-fueled power plants are major GHG emission sources while solar and wind resources do not emit GHG at all in daily operations. The GHG emission from power systems is influenced by many factors [3] such as generation mix, time of the day, season, electric load level, and the topology of the power system.

This work was supported by the National Science Foundation award 2324940 and California Energy Commission award GFO-19-309.

To reduce GHG emissions, accurate GHG emission predictions are in critical need. There are two major GHG emission factors: average emissions factor (AEF) and marginal emissions factor (MEF). The AEF is calculated as the ratio of total GHG emissions to the total power consumption. The MEF is the ratio of the change of GHG emissions to the change of power consumption. Compared with AEF, MEF is a more useful tool for distributed energy resources aggregators and end-use customers to make intelligent decisions about how much electricity should be consumed at different time slots of a day. MEF signals can be sent along with electricity prices signals to flexible loads and other smart technologies of the residential, commercial and industrial customers [4]. Based on the MEF signals, flexible loads, such as electric vehicles (EVs), smart thermostats, and batteries can consume or charge less power during high MEF hours and more power during low MEF hours. MEF can also be considered in new electricity pricing design to help reduce GHG emissions.

GHG emission and marginal GHG emission prediction methods are in their early stage of research and development. The existing methods can be classified into three groups. In the first group, GHG emission or MEF is estimated through production cost simulations of power systems and electricity markets. Reference [3] used load duration curve and economic dispatch to emulate power plants dispatch. In [5], the order of dispatching was empirically derived to calculate AEF and MEF. In [6], simulations in detailed transmission system models were used to estimate GHG emissions. These approaches have two drawbacks. First, to accurately predict AEF or MEF, high-fidelity production cost simulations of electricity markets are needed. This can be computationally expensive if MEF needs to be calculated at high granularity in space and time. Second, only the market operators have access to accurate models of transmission networks and propriety bids and offers submitted by power producers and load serving entities, making it difficult for others to apply these methods.

The second group of methods are based on clustering and linear regression. In [7], [8], linear regression was used to predict GHG emissions from load. In [9], cluster analysis

979-8-3503-9678-2/23/$31.00 ©2023 IEEE

was first conducted on daily load curves and linear regression models were developed for each cluster to predict MEF. The drawback of these approaches is that linear regression models can not accurately capture the complex interactions between different influential factors in determining GHG emissions.

In the third group, machine learning models such as feed-forward neural networks (FNNs) [10], [11], support vector machines (SVMs) [12], and long short-term memory (LSTM) networks [11] were proposed to predict GHG emissions. In [13], an ensemble model combining multiple basic models such as FNN, LSTM, and random forest (RF) was trained to predict GHG emissions. Although machine learning models have shown good prediction accuracy, most of them were designed to do long-term predictions with very low time granularity, such as yearly GHG emissions, which are not sufficient for short-term control of flexible loads and smart buildings. Furthermore, these models were designed separately to forecast GHG emissions in each region, ignoring the interactions between different load serving zones, which greatly limited the prediction accuracy.

The marginal GHG emission factor varies by load zones, or electric buses, due to the limited power transfer capability between zones and nodes in the power system. To accurately predict the locational MEF, the information from the entire transmission network should be effectively leveraged. Graph neural network (GNN) [14], [15] is an ideal candidate for processing and learning from information collected from a complex network such as the power grid. In fact, GNN has received increasing attention in recent years from researchers to tackle a number of prediction, estimation and optimization problems in power systems such as optimal power flow [16], solar energy prediction [17], parameter estimation [18], state estimation [19], and system health index prediction [20].

In this paper, we propose a hybrid machine learning model, which integrates FNNs with spatio-temporal graph convolutional networks (STGCNs) [21] to predict GHG emissions and the MEF. We adopted the STGCN due to its capability to efficiently capture temporal and spatial structure of the network data. Compared with existing GHG emission prediction methods, our proposed model has three advantages. First, it captures the complex interactions between multiple load zones and thus provides highly accurate locational MEF prediction. Second, it provides short-term MEF predictions with hourly granularity to aggregators and end-users to control flexible loads. Third, the model uses only publicly available electricity market and power system information, making it widely applicable. A comprehensive case study in California electricity market shows that the proposed method has more accurate predictions of GHG emissions and MEF than baseline methods.

The rest of the paper is organized as follows. Section II describes the problem setup and the dataset. Section III presents the technical details of the proposed hybrid machine learning model. Section IV evaluates the GHG emission prediction performance and the analyzes the MEF in different scenarios. Section V states the conclusion.

II. Problem Setup and Dataset Description

A. Problem Setup

The objective of this work is to obtain an accurate prediction of GHG emissions as well as locational MEF of electricity. Let $E_t(x_{1t}, x_{2t}, ..., x_{Rt})$ be the GHG emission of a system at time t with influential factors $x_{1t}, x_{2t}, ..., x_{Rt}$. x_{rt} is the load of a subsystem r at time t. Then the locational MEF due to a local load change Δx at subsystem r at time t is defined in (1). If the GHG emission is measured in metric ton of carbon dioxide equivalent per hour ($mTCO_2/h$) and the load is measured in megawatt (MW), then the MEF is measured in $mTCO_2/MWh$.

$$\frac{\Delta E}{\Delta G} = \frac{E_t(x_{1t}, ..., x_{rt}+\Delta x, ..., x_{Rt}) - E_t(x_{1t}, ..., x_{rt}, ..., x_{Rt})}{\Delta x} \tag{1}$$

The prediction of GHG emissions and locational MEF are conducted in two steps. First, machine learning models are trained to predict GHG emissions based on electric power load and other input features. Second, machine learning models are used to make new GHG emission predictions with perturbed load levels. The locational MEF is then calculated following the definition in (1).

B. Description of the Dataset

In this paper, we used real-world GHG emissions of California in the test case. We utilized data from six sources, which are summarized in Table I. All of the data, except time, were collected from the Open Access Same-time Information System (OASIS) of the California Independent System Operator (CAISO), which is publicly-available [22]. In the dataset, CAISO measured GHG emissions by tracking the power generations of power plants, the heat rate provided by generation asset owners, and the GHG emission factors by resource types [23]. The data were collected between July 2018 and September 2022. After data cleansing and preprocessing, about 37,000 hours of data remained.

TABLE I: Summary of Input and Output Data

	Data Type
Input	Day-ahead hourly electric load predictions of different balancing authorities (MWh).
	Two day-ahead predictions of solar and wind power generation of different regions (MWh).
	Hourly natural gas price of different regions (dollars per thousand cubic feet).
	Hourly power supply from different generation resources: renewables, natural gas, large hydro, imports, batteries, nuclear, and coal (MWh).
	Time: month, hour, weekday/weekend.
Output	Total hourly California power grid emission from all resources: imports, natural gas, biogas, biomass, geothermal, and coal ($\mathrm{mTCO_2}$)

The electric load data were collected from not only California, but also other parts of western United States. These regions and the corresponding balancing authorities are summarized in Table II and their locations are illustrated in Fig. 1. All the load data used were one day-ahead predictions made by

system operators with mean absolute percentage error (MAPE) below 3%.

TABLE II: Summary of the Regions and Balancing Authorities of the Load Data

Code Name	Full Name	State
MWD-TAC	Metropolitan Water District Transmission System	California
PGE-TAC	Pacific Gas And Electric	California
SCE-TAC	Southern California Edison	California
SDGE-TAC	San Diego Gas And Electric	California
VEA-TAC	Valley Electric Association	California
IPCO	Idaho Power Company	Idaho
PACE	PacifiCorp East	Utah
PACW	PacifiCorp West	Utah
PGE	Portland General Electric	Oregon
PSEI	Puget Sound Energy	Washington
NEVP	Nevada Energy	Nevada

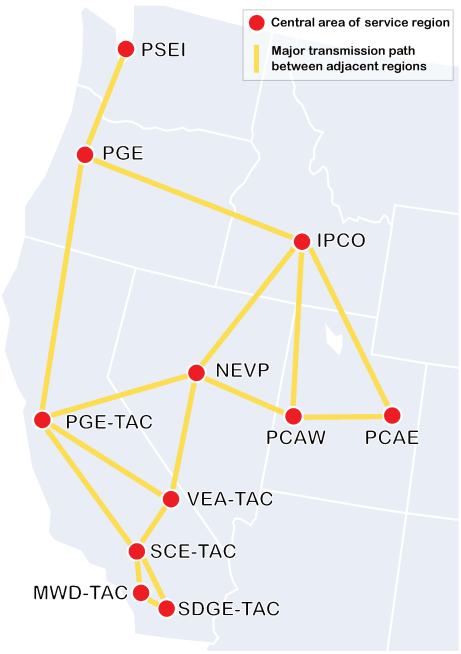

Fig. 1: Electric power interconnection map

The solar and wind power generation data in California were from three regions (coded as NP15, ZP26, and SP1) specified by CAISO, which represent the north, middle, and south of California. They were two day-ahead predictions made by CAISO with MAPE below 7%. Natural gas is the main fuel source for thermal power plants in California, and thus its price in different regions of California was collected. The power supply by resource type reported by CAISO are used as input features. The output of the prediction model is the total GHG emissions of all the electric power resources in California.

III. Technical Methodology

A. Overall Framework of the GHG Emission Prediction Model

The overall framework of the proposed GHG emission prediction model is illustrated in Fig. 2. As shown in the figure, we design a hybrid model that combines both STGCNs and FNNs. The load graph block and the renewable generation graph block are two STGCN models, while the parallel block is an FNN model. The load data and the renewable generation data are fed into the load graph block and renewable generation graph block respectively; these two types of data and other input data are also fed into the parallel block. The outputs of these three blocks are concatenated into one tensor for each time instance, and fed into the output block, which is an FNN network and its output is the predicted GHG emission. The details of the proposed method is described in the following subsections, including the data preprocessing, brief introduction of STGCN, the design of each block, and the data split and hyperparameter tuning.

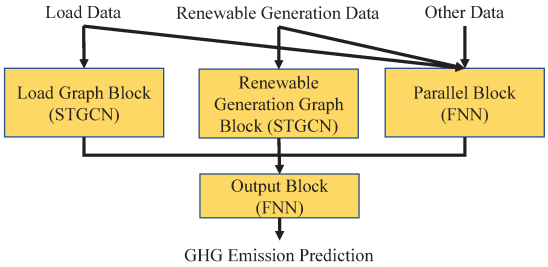

Fig. 2: Framework of the Prediction Model

B. Data Preprocessing

1) Preprocessing of Time Data: We used a binary variable to represent weekday (value 0) and weekend (value 1). To represent month and hour, we use cyclical encoding. In cyclical encoding, The k-th hour ($k = 1, 2, ..., 24$) is encoded by $[cos\frac{2\pi k}{24}, sin\frac{2\pi k}{24}]$. Similarly, the k-th month ($k = 1, 2, ..., 12$) is encoded by $[cos\frac{2\pi k}{12}, sin\frac{2\pi k}{12}]$.

2) Transformation of Data: To improve the convergence in training and prediction accuracy, we applied two types of transformation to the data: z-score normalization and quantile transformation. In the z-score normalization, the data are centered and normalized by their standard deviation. In the quantile transformation, the data are transformed to follow a normal distribution. The z-score normalization is a linear transformation, which preserves the correlations and distances within the data; on the other hand, the nonlinear quantile transformation smooths out unusual distributions and is less influences by outliers than z-score.

C. Brief Introduction of STGCN

Here we briefly introduce the design of STGCN and more details can be found in [21]. STGCN is designed to process and learn data set collected from a graph. Let $\mathcal{G} = (\mathcal{V}, \mathcal{E}, W)$ be a graph, in which $\mathcal{V}$ is the set of vertices (nodes), $\mathcal{E}$ is the set of edges, and $W \in \mathbb{R}^{n \times n}$ is the weighted adjacency matrix ($n = |\mathcal{V}|$). The structure of the STGCN model is illustrated in Fig. 3. An STGCN contains three parts: two spatial-temporal convolutional (ST-Conv) blocks and an output layer. Each ST-Conv block contains a "sandwich" structure of two temporal

gated convolution (Gated-Conv) layers and one spatial graph convolution (Graph-Conv) layer. The output layer is a fully connected layer.

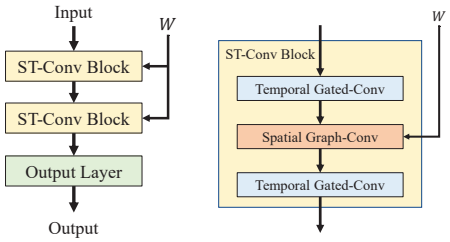

(a) STGCN (b) ST-Conv

Fig. 3: The structure of an STGCN model. (a) is the overall structure of STGCN. (b) is the internal structure of an ST-Conv block.

The Graph-Conv layer uses Chebyshev polynomials to approximate a graph convolution operation "$*\mathcal{G}$" with a kernel Θ as defined in (2):

$$\Theta_{*\mathcal{G}}\boldsymbol{x} = \Theta(L) \approx \sum_{k=0}^{K-1} \theta_k T_k(\tilde{L})\boldsymbol{x} \tag{2}$$

Here, $T_k(\tilde{L}) \in \mathbb{R}^{n\times n}$ is the Chebyshev polynomial of order k, $\tilde{L} = 2L/\lambda_{max} - I_n$ is the scaled Laplacian, and $\boldsymbol{x}$ is a n-dimensional vector representing the inputs at the graph nodes. $L = I_n - D^{-\frac{1}{2}}WD^{-\frac{1}{2}}$. I_n is an identity matrix. $D \in \mathbb{R}^{n\times n}$ is the diagonal degree matrix derived from W, and λ_{max} is the largest eigenvalue of L. K is the kernel size, which determines the maximum radius of the convolution. When each node has a C_i-channel input and C_o-dimensional output, the graph is generalized to (3):

$$\boldsymbol{y}_j = \sum_{i=1}^{C_i} \Theta_{i,j}(L)\boldsymbol{x}_i \in \mathbb{R}^n, 1 \le j \le C_o \tag{3}$$

Here $\boldsymbol{y}_j \in \mathbb{R}^n$ is the nodal output of channel j. $\boldsymbol{x}_i \in \mathbb{R}^n$ is the nodal input of channel i. When multiple time steps are considered, the input and output will have an additional dimension for time steps.

The temporal Gated-Conv layer is applied to each node in the graph. Let M be the input time steps; let C_i and C_o be numbers of the input and output channels. The Gated-Conv layer first uses a convolution kernel $\Gamma \in \mathbb{R}^{K_t\times C_i\times 2C_o}$ to perform 1-D causal convolutions of width K_t and obtains two elements P and Q, such that $[P, Q] \in \mathbb{R}^{(M-K_t+1)\times(2C_o)}$. Then this layer uses element-wise Hadamard product ($\odot$) to obtain its out as $P \odot \sigma(Q) \in \mathbb{R}^{(M-K_t+1)\times C_o}$, where $\sigma()$ is the sigmoid gate.

D. Load Graph Block

To process the load data with a STGCN model, we need to determine the graph, model structure, the inputs and outputs of the model. We use the graph shown in Fig. 1, in which each node represents a balancing authority and each edge represents a major transmission path between adjacent regions. We construct the adjacency matrix W for the model by using the same weight for each edge in the graph. We use a single-step in both the inputs and outputs of the STGCN. Thus, in the temporal Gated-Conv layers, we set $K_t = 1$. We assume that each region have direct interactions with only its nearest neighbors, thus we use a maximum radius of 1 in the Spatial Graph-Conv layer, i.e. $K = 2$. To predict the GHG emission at hour h, the inputs of each node in this graph are the load at hour h and $h - 24$ of the corresponding region with both the z-score and quantile transformation. Note that load used here are all one day-ahead predictions.

E. Renewable Generation Graph Block

Similar to the load data, the renewable generation data of solar power and wind power also have a graph structure. The renewable generation data was recorded separately in the three regions: NP15, ZP26, and SP15, representing the north, central, and the south parts of California. Thus, the graph of this block was designed as three nodes connected to each other with three edges. We use a single time step in both the input and output, thus we set $K_t = 1$. Since it is a small graph, any non-zero convolution radius will average the nodal features. Hence, we set $K = 1$ to avoid this. To predict the GHG emission at hour h, the inputs of this block are the renewable generation power at hour h and $h - 24$ with both the z-score and quantile transformation for each of the three nodes. Note that the renewable generation data used here are all two day-ahead predictions.

F. Parallel Block

Since not all input data are collected from a graph, we also design a parallel block to extract information that is not captured by the STGCN blocks. The inputs to the parallel block include the load data, renewable generation data an other input data. The other input data are the time feature data (described in Section III-B) of hour h and $h - 24$, the natural gas price at hour h and $h - 24$, the supply resource mix at hour $h - 24$, and the historical GHG emission at hour $h - 24$. Every input feature except time and historical GHG emission uses both z-score and quantile transformation. The historical GHG emission uses only the quantile transformation.

G. Output Block

The output block is designed as an FNN with batch normalization before each layer. Its output is the quantile transformation of the GHG emission. The proposed hybrid model is trained to minimize the mean squared error of the quantile-transformed GHG emission. To obtain the final prediction, inverse of quantile transform is performed.

H. Data Split and Hyperparameter Tuning

To train the proposed model and tune its hyperparameters, the dataset is split into three parts. The first 80% of samples are used as the training and validation dataset while the last 20% of the samples were used as the testing dataset to evaluate the model's GHG emission prediction performance. In the first

80% of samples, for every five day's data (120 samples), we put the first four days into the training dataset and the last day's data into the validation dataset. Thus, 64% of the whole data set is used as the training dataset and 16% is used as the validation dataset. The proposed machine learning model contains many hyperparameters: the number of layers in each block, the dimension of each layer, the size of spatial kernel and temporal kernel, learning rate, etc. To systematically tune hyperparameters, for each hyperparameter setup, we trained the model 10 times using the training dataset, and calculate the average prediction error using the validation dataset. The hyperparameter setup with the lowest average error in the validation dataset is chosen as the best hyperparameter setup.

IV. GHG Emission Prediction Performance and Analysis of Marginal GHG Emission

In this section, we evaluate the prediction performance for California's GHG emissions of the proposed hybrid machine learning model and compared it with two baseline algorithms. We also calculate and analyze the locational MEF under different scenarios.

A. GHG Emission Prediction Performance

We compare the GHG emission prediction performance of our proposed model (hybrid STGCN) and two other baseline models: FNN and gradient boosted trees (GBT). Note that the FNN and GBT models use the same input features as our proposed model.

The hyperparameters all three machine learning models were tuned following the approach in Subsection III-H. We trained the hybrid STGCN model and FNN model using the Adam algorithm, with batch size $= 10$ and early stopping patience $= 10$ epochs. We trained the GBT with early stopping patience $= 10$ rounds. By tuning hyperparameters, the numbers of channels of the three "sandwich" layers in ST-Conv and the output layer of STGCN are $4-2-4-2$ respectively in the load graph block, and $8-4-8-2$ in the renewable generation graph block; the FNN in the parallel block and the output block are two three-layer FNNs of dimension 20–20–1. The number of neurons of the FNN model is $20-20-20-1$. All FNN models use batch normalization before each layer.

To evaluate the prediction accuracy of the machine learning models, we train each model 10 times using the training dataset, and then test the models with the testing dataset. Three error metrics are used to evaluate the prediction accuracy: mean squared error (MSE), mean absolute error (MAE), and mean absolute percentage error (MAPE). The prediction performance of the three machine learning models are compared in Table III. For each type of measurements, two values were recorded: the average performance over 10 tests, and the optimal value, i.e. the performance of the model with the lowest validation loss. We can see that our proposed hybrid STGCN model has the lowest prediction error in MSE, MAE, and MAPE in both average value and the optimal value. In addition, by choosing the optimal value from multiple trained models, our proposed prediction model can further improve the prediction accuracy. These results show that by capturing the complex spatio-temporal relationship of the data, our proposed model can significantly improve the accuracy of GHG emission prediction.

TABLE III: Prediction Performance of GHG Emissions. (Average Value / Optimal Value)

Model	MSE $(mTCO_2/h)^2$	MAE $(mTCO_2/h)$	MAPE (%)
Hybrid STGCN	2.90/2.77E+05	4.02/3.88E+02	9.46/9.15
FNN	3.01/3.11E+05	4.09/4.18E+02	10.80/10.36
GBT	3.25/3.23E+05	4.27/4.25E+02	11.43/11.43

B. Analysis of Locational Marginal GHG Emission

We use the trained hybrid STGCN model to calculate the locational MEF and ΔE, following the definition in (1). The locational MEF and ΔE are calculated for each hour and each region's load change in the dataset, with a $\Delta G = 100MW$. We then analyze the locational marginal MEFs in two aspects: hourly pattern of locational MEF with high renewable energy output and weekday/weekend effect.

1) Locational MEF on a Day with High Renewable Energy Output: California has very high renewable energy penetration rate. On March 27, 2022, California hit a record that 94.5% of the electricity on the grid came form renewable energy [24]. We calculate the 24-hour locational MEF on this day in the balancing authority of PGE-TAC and SCE-TAC respectively. The result is illustrated in Fig. 4. From this figure, we can see that the marginal GHG emission is significantly lower during the day. This is because solar photovoltaic (PV) generation is very high during these hours and does not emit any GHG. This result shows that the proposed hybrid STGCN model successfully recognizes the contribution of renewable energy in reducing GHG emission. Furthermore, the MEF for SCE-TAC and slightly lower than that of PGE-TAC between 12:00 pm and 18:00 pm. This is because Southern California has much higher solar PV generation and not all all renewable energy can be moved from Southern California to Northern California due to limited power transfer capability.

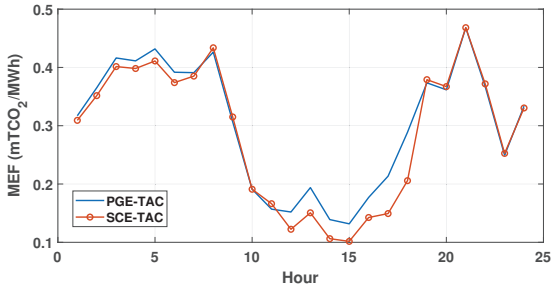

Fig. 4: Hourly MEF on March 27, 2022 for PGE-TAC and SCE-TAC.

2) Weekday/Weekend Effect on Marginal GHG Emission: We calculate the average locational MEF for 24 hours on weekdays and weekends in the PGE-TAC area. The result is

illustrated in Fig. 5. From this figure, we can see that the MEF is lower during the day, which has been explained in Subsection IV-B1. We can also observe that the weekends have lower MEF than the weekdays. This is due to the lower power demand on weekends. When there are lower power demand, system operators can turn off the less fuel-efficient power stations and keep running the power plants with higher fuel-efficiency. These results show that the proposed hybrid STGCN model can reflect the GHG emission differences between weekday and weekends and between different operation conditions.

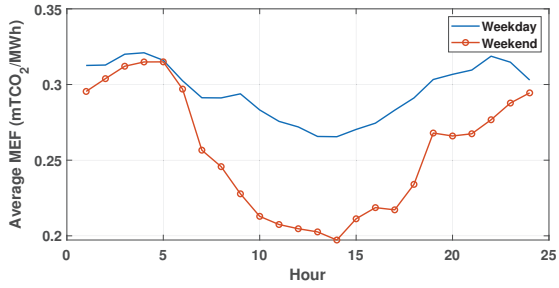

Fig. 5: Average hourly MEF on weekdays/weekends in PGE-TAC.

V. Conclusion

In this paper, we developed a hybrid machine learning model by integrating FNN with STGCNs to predict GHG emissions and locational MEF. The STGCN components of the model allows us to capture the complex spatio-temporal correlations in the network data and improves the prediction accuracy. The proposed model can provide short-term locational MEF predictions at hourly granularity to aggregators and end-users to manage flexible loads and it does not require accurate power system model. The numerical study on California's electricity market shows that the proposed method has more accurate GHG emission predictions than the baseline machine learning models. Detailed analysis also showed how the locational MEF is influenced by load level, hour, and renewable generation levels.

References

[1] The White House, "Fact sheet: President Biden sets 2030 greenhouse gas pollution reduction target aimed at creating good-paying union jobs and securing U.S. leadership on clean energy technologies," April 2022.

[2] U.S. Environmental Protection Agency, "Sources of greenhouse gas emissions," August 2022. [Online]. Available: https://www.epa.gov/ghgemissions/sources-greenhouse-gas-emissions

[3] C. Marnay, D. C. Fisher, S. Murtishaw, A. A. Phadke, L. K. Price, and J. A. Sathaye, "Estimating carbon dioxide emissions factors for the California electric power sector," *Proceedings of the 2002 ACEEE's Summer Study on Energy Efficiency*, vol. 33, no. 99, 2002.

[4] WattTime, "Marginal emissions modeling: WattTime's approach to modeling and validation," Oct 2022. [Online]. Available: https://www.watttime.org/app/uploads/2022/10/WattTime-MOER-modeling-20221004.pdf

[5] R. Bettle, C. H. Pout, and E. R. Hitchin, "Interactions between electricity-saving measures and carbon emissions from power generation in england and wales," *Energy Policy*, vol. 34, no. 18, pp. 3434–3446, 2006.

[6] D. L. Shawhan, J. T. Taber, D. Shi, R. D. Zimmerman, J. Yan, C. M. Marquet, Y. Qi, B. Mao, R. E. Schuler, W. D. Schulze, and D. Tylavsky, "Does a detailed model of the electricity grid matter? Estimating the impacts of the regional greenhouse gas initiative," *Resource and Energy Economics*, vol. 36, no. 1, pp. 191–207, 2014.

[7] A. Hawkes, "Estimating marginal CO_2 emissions rates for national electricity systems," *Energy Policy*, vol. 38, no. 10, pp. 5977–5987, 2010.

[8] K. Siler-Evans, I. L. Azevedo, and M. G. Morgan, "Marginal emissions factors for the U.S. electricity system," *Environmental Science & Technology*, vol. 46, no. 9, pp. 4742–4748, 2012.

[9] D. S. Callaway, M. Fowlie, and G. McCormick, "Location, location, location: The variable value of renewable energy and demand-side efficiency resources," *Journal of the Association of Environmental and Resource Economists*, vol. 5, no. 1, pp. 39 – 75, 2018.

[10] L.-N. Guo, C. She, D.-B. Kong, S.-L. Yan, Y.-P. Xu, M. Khayatnezhad, and F. Gholinia, "Prediction of the effects of climate change on hydroelectric generation, electricity demand, and emissions of greenhouse gases under climatic scenarios and optimized ANN model," *Energy Reports*, vol. 7, pp. 5431–5445, 2021.

[11] L. Alfaseeh, R. Tu, B. Farooq, and M. Hatzopoulou, "Greenhouse gas emission prediction on road network using deep sequence learning," *Transportation Research Part D: Transport and Environment*, vol. 88, p. 102593, 2020.

[12] M. S. Bakay and Ümit Ağbulut, "Electricity production based forecasting of greenhouse gas emissions in Turkey with deep learning, support vector machine and artificial neural network algorithms," *Journal of Cleaner Production*, vol. 285, p. 125324, 2021.

[13] M. Emami Javanmard and S. Ghaderi, "A hybrid model with applying machine learning algorithms and optimization model to forecast greenhouse gas emissions with energy market data," *Sustainable Cities and Society*, vol. 82, p. 103886, 2022.

[14] J. Zhou, G. Cui, S. Hu, Z. Zhang, C. Yang, Z. Liu, L. Wang, C. Li, and M. Sun, "Graph neural networks: A review of methods and applications," *AI open*, vol. 1, pp. 57–81, 2020.

[15] T. N. Kipf and M. Welling, "Semi-supervised classification with graph convolutional networks," in *2017 International Conference on Learning Representations (ICLR)*, April 2017, pp. 1–11.

[16] D. Owerko, F. Gama, and A. Ribeiro, "Optimal power flow using graph neural networks," in *ICASSP 2020 IEEE International Conference on Acoustics, Speech and Signal Processing (ICASSP)*, 2020, pp. 5930–5934.

[17] A. M. Karimi, Y. Wu, M. Koyuturk, and R. H. French, "Spatiotemporal graph neural network for performance prediction of photovoltaic power systems," in *Proceedings of the AAAI Conference on Artificial Intelligence*, vol. 35, no. 17, 2021, pp. 15 323–15 330.

[18] W. Wang and N. Yu, "Estimate three-phase distribution line parameters with physics-informed graphical learning method," *IEEE Trans. Power Syst.*, vol. 37, no. 5, pp. 3577–3591, 2022.

[19] Q. Yang and A. Sadeghi, "Graph convolutional networks for power system state estimation," in *2020 IEEE International Conference on Communications, Control, and Computing Technologies for Smart Grids (SmartGridComm)*, 2020.

[20] K. Yamashita, J. Qin, N. Yu, E. Farantatos, and L. Zhu, "Predicting power system voltage health index with PMUs and graph convolutional networks," in *2023 IEEE Power & Energy Society General Meeting (PESGM)*, 2023.

[21] B. Yu, H. Yin, and Z. Zhu, "Spatio-temporal graph convolutional networks: A deep learning framework for traffic forecasting," *Proceedings of the 27th International Joint Conference on Artificial Intelligence*, no. 7, p. 3634–3640, 2018.

[22] California Independent System Operator (CAISO), "Open access same-time information system (OASIS)." [Online]. Available: http://oasis.caiso.com/mrioasis/logon.do

[23] A. Hundiwale, "Greenhouse gas emission tracking methodology," California Independent System Operator, Tech. Rep., 2016. [Online]. Available: http://www.caiso.com/Documents/GreenhouseGasEmissionsTracking-Methodology.pdf

[24] California Independent System Operator (CAISO), "California ISO hits all-time peak of more than 97% renewables," April 2022. [Online]. Available: https://www.caiso.com/Documents/California-ISO-Hits-All-Time-Peak-of-More-Than-97-Percent-Renewables.pdf